Photolysis of Disilane at 193 nm

Naoya Tada, Kenichi Tonokura, Keiji Matsumoto, Mitsuo Koshi,* Akira Miyoshi, and Hiroyuki Matsui

Department of Chemical System Engineering, The University of Tokyo, 7-3-1 Hongo, Bunkyo-ku, Tokyo 113-8656, Japan

Received: May 22, 1998; In Final Form: October 14, 1998

The primary photochemical process of Si_2H_6 at 193 nm has been studied by using time-resolved mass spectrometry and laser-induced fluorescence (LIF) techniques. Si_2H_2 was confirmed as a primary photoproduct, but no signal due to SiH_3, Si_2H_3, Si_2H_4, and Si_2H_5 in 193 nm photolysis has been detected. SiH_2 was observed in a pump-and-probe experiment by the LIF method, which rapidly reacts with the Si_2H_6 parent molecule to form Si_3H_8. The quantum yield of Si_3H_8 produced in the reaction of $SiH_2 + Si_2H_6$ was estimated to be 0.13 $\pm$ 0.02 by using electron impact mass spectrometry. It was concluded that SiH_2 produced by the photolysis exclusively reacted with Si_2H_6 and thus the quantum yield of SiH_2 was equal to that of Si_3H_8, i.e., 0.13. The quantum yield of H atom was estimated to be 0.09 $\pm$ 0.01 by using vacuum ultraviolet (VUV) LIF. On the basis of the existing data and present results, it was suggested that the H_2 molecule production channels are dominant in 193 nm photolysis of Si_2H_6.

1. Introduction

Si_2H_6 photochemistry is of fundamental importance in photochemical vapor deposition (photo-CVD) to form hydrogenated amorphous silicon (a-Si:H). The absorption cross section of Si_2H_6 at 193 nm, $\sigma \approx 3.4 \times 10^{-18}$ cm^2,[1] is quite suitable for laser-induced CVD (LCVD) by a 193 nm ArF excimer laser. Understanding the gas-phase photochemistry of Si_2H_6 is critical to clarify the mechanism of Si thin film growth in LCVD. Thus, the photodissociation processes of Si_2H_6 at 193 nm have been studied extensively by various experimental techniques.[1−7] In 193 nm photolysis of Si_2H_6, 21 dissociation pathways are energetically possible[8] since one 193 nm photon (148 kcal/mol) provides enough energy to break any single bond in Si_2H_6 and numerous combinations of bonds, as summarized in Table 1.

Direct measurements of the photoproducts have been performed to understand the primary photochemistry of Si_2H_6 at 193 nm by many researchers. Chu et al.[1] determined the total quantum yield for loss of Si_2H_6 and the quantum yield for the formation of SiH_4 by using time-resolved infrared diode laser absorption spectroscopy. Okada et al.[6] reported the quantum yield of Si atom formation by [2 + 1] resonance-enhanced multiphoton ionization (REMPI) and detection of Si_2 and SiH radicals by laser-induced fluorescence (LIF) technique. It has been proposed that disilicon species such as H_3SiSiH or H_2SiSiH_2 produced by 193 nm photolysis of Si_2H_6 may play a key role in the LCVD.[1,2,7] There are arguments with respect to the formation of SiH_2 in 193 nm photolysis of Si_2H_6. No SiH_2 has been detected by using intracavity laser spectroscopy[3] and LIF methods.[6] On the other hand, 193 nm photolysis of Si_2H_6 was used as a source of SiH_2 radical in the kinetics experiment.[9] Thus, there still remain opacities in the primary photochemical processes at 193 nm.

Contrary to 193 nm photolysis, the quantum yields for the stable products at 147 nm were well established, although the nature of the primary processes is speculative. The study of Si_2H_6 photochemistry at 147 nm has been performed by Perkins and Lampe by the observation of photoproducts during continuous irradiation of the sample with a Xe resonance lamp.[10] They detected H_2, SiH_4, Si_3H_8, Si_4H_{10}, Si_5H_{12}, and a solid hydridic silicon film. Three primary processes ($SiH_2 + SiH_3 + H$, ϕ = 0.61; $SiH_3SiH + 2H$, $\phi = 0.18$; $Si_2H_5 + H$, $\phi = 0.21$) out of a total of 39 pathways were proposed to account for the observed quantum yields of these species.

In the present study, the photochemical decomposition mechanism of Si_2H_6 at 193 nm is examined in detail by using time-resolved mass spectrometry and LIF techniques, providing the basis to understand the LCVD. The primary photochemical processes of Si_2H_6 at 193 nm are proposed on the basis of the quantitative results. The results are remarkably different from the photochemical decomposition mechanism at 147 nm.

2. Experimental Section

Mass Spectrometry Experiments. Two mass spectrometric techniques were used in the present study, electron impact ionization mass spectrometry (EI-MS) and photoionization mass spectrometry (PI-MS).

The experimental setup for EI-MS is the same as that used for our previous study.[11] The reactant gas mixtures were slowly flowed into a Pyrex photolysis cell and were irradiated by an unfocused ArF excimer laser beam (Questek 2220 or Lambda Physik, Compex 102). The photoproducts were continuously sampled through a pinhole of about 250 μm in diameter into an electron impact ionization chamber of the quadrupole mass spectrometer (Anelva, AQA-200). The mass-selected signal was detected by a two-stage microchannel plate (MCP), which was operated under pulse-counting conditions. The pulse signal was sent into a gated counter, and the time dependence at a fixed mass number was obtained by scanning the delay time of the gate with a fixed gate width of 100 μs. Signals were accumulated over 2000−20000 laser shots. The gas pressures were measured with a capacitance manometer (MKS Baratron, 122A). The chamber was pumped by a 600 L/s diffusion pump with a liquid

* Corresponding author. E-mail: koshi@chemsys.t.u-tokyo.ac.jp.

10.1021/jp982348a CCC: $18.00
Published on Web 01/14/1999

TABLE 1: Energetics of Dissociation Processes of Si_2H_6 at 298 K[a]

ground-state products	ΔH kcal/mol		excited-state products	ΔH kcal/mol	
$H_2SiSiH_2 + H_2$	38.0	(r1)	$H_2SiSiH_2(^3B) + H_2$	72.9	(r16)
$SiH_4 + SiH_2$	57.8	(r2)	$SiH_4 + SiH_2(\tilde{a}^3B_1)$	77.4	(r17)
$H_3SiSiH + H_2$	61.3	(r3)	$SiH_4 + SiH_2(\tilde{A}^1B_1)$	102.1	(r18)
$Si(H_2)Si + 2H_2$	70.4	(r4)	$SiH_4 + Si(3p^1D_2) + H_2$	114.8	(r19)
$2SiH_3$	76.5	(r5)	$SiH_2(\tilde{a}^3B_1) + SiH_2 + H_2$	137.9	(r20)
$H_2SiSi + 2H_2$	85.3	(r6)	$SiH_4 + Si(3p\ ^1S_o) + H_2$	140.7	(r21)
$H_3SiSiH_2 + H$	88.7	(r7)			
$SiH_4 + Si + H_2$	96.8	(r8)			
$2SiH_2 + H_2$	118.3	(r9)			
$SiH_3 + SiH_2 + H$	120.7	(r10)			
$Si_2 + 3H_2$	121.9	(r11)			
$SiH_4 + SiH + H$	133.2	(r12)			
$H_2SiSiH + H_2 + H$	138.8	(r13)			
$H_2SiSiH_2 + 2H$	142.2	(r14)			
$Si(H)Si + 2H_2 + H$	148.8	(r15)			

[a] Taken from ref 8.

nitrogen trap to a base pressure of 2×10^{-7} Torr. The pressure in the chamber was kept at $(5-7) \times 10^{-6}$ Torr during the experiment. The ionization energies used in the present study are 15 (H_2), 11 (Si_2H_2), 10 (Si_2H_4), and 16 eV (Si_3H_8).

The apparatus for PI-MS is the same as that reported previously.[12] The gas mixtures flowing through a Pyrex cell were irradiated by a 193 nm excimer laser (Lambda Physik, LEXtra 50SL). A small part of the photolyzed gas was introduced into a photoionization chamber through a 200 μm pinhole. The reaction products were photoionized by a H (10.2 eV), O (9.5 eV), and Cl (8.9 eV) resonance lamp powered by a microwave discharge and were mass-selected by a quadrupole mass filter (ULVAC, MSQ-150A). Temporal signal was detected by a secondary electron multiplier (SEM; Hamamatsu, R924), which was operated under pulse-counting conditions. The pulse signal was sent into a discriminator, and the time dependence at a fixed mass number was obtained by scanning the delay time of the gate with a fixed gate width of 100 μs. Signals were accumulated over 2000−10000 laser shots.

Laser-Induced Fluorescence (LIF) Experiments. The experimental apparatus used for LIF studies is essentially same as the system used for the previous work.[13] H atoms were detected by a VUV LIF technique at the Lyman α wavelength (121.6 nm). The probe light for H atoms at 121.57 nm was generated by frequency tripling in a Kr cell. The 364.6 nm laser light (6−10 mJ/pulse) was generated by the output of an excimer pumped dye laser (Lambda Physik, LPX 110i and Lambda Physik, LPD 3002). The UV laser light was focused with an axisymmetric quartz lens ($f = 7$ cm) into the tripling cell (14 cm in length). The intensity of the vacuum UV light going through a reaction cell was monitored behind the reaction cell by using an ionization cell filled with 2% NO diluted in He at a total pressure of 20 Torr. The tripling cell and ionization cell were directly connected to the reaction cell through a LiF window. The vacuum UV LIF signal was observed by a solar-blind photomultiplier (Hamamatsu, R972) at right angles to both the photolysis and probe lasers through the LiF window.

The $SiH_2(\tilde{X}^1A_1)$ produced in 193 nm photolysis was observed by LIF on the $\tilde{A}^1B_1 \leftarrow \tilde{X}^1A_1$ transition of (0,2,0)−(0,0,0) and (0,3,0)−(0,0,0) bands at the wavelength ranges of 578−583 and 550−555 nm, respectively.[14] The visible laser light was obtained by the same excimer pumped dye laser. The LIF signal was detected by a photomultiplier (Hamamatsu, R105) and amplified by a preamplifier (NF, BX-31). A band-pass filter or interference filter was put in front of the photomultiplier to minimize scattered light from 193 nm laser and luminescence resulting from photolysis. The probe laser power was monitored by a PIN photodiode during experiments. The intensity of the LIF signals and probe laser power were averaged with boxcar integrators (Stanford Research, SR250) and stored in a microcomputer for further data analysis.

Experimental Conditions. Kinetics and spectroscopic measurements were carried out at a laser repetition of 7−9 Hz to ensure complete removal of the reacted mixture and replenishment of the gas sample between successive laser shots. The 193 nm laser intensity used was typically 15 mJ cm^{-2} per pulse. On the basis of the photoabsorption cross section of 3.4×10^{-18} cm^2 for Si_2H_6 and the photon density we used, initial concentrations of short-lived species produced by the photolysis are estimated to be less than 10^{12} molecules cm^{-3}. In the quantum yield measurements, the fraction of light absorbed by Si_2H_6 is about 3−5%. We have confirmed that the photolysis laser power dependence of the signals was first order in the range of 10−50 mJ/cm^2 per pulse. Therefore, multiphoton excitation of the parent molecule and secondary dissociation of the photoproducts may be ruled out. In this study, the quantum yields per quantum absorbed were determined. In the quantum yield measurements of Si_3H_8, the uncertainty of 10% is evaluated from the photon density measurements, and the concentration of Si_2H_6 used was in the range of $(0.1-5) \times 10^{14}$ molecules cm^{-3}. Experiments were carried out at room temperature (297 ± 2 K) with total pressures of $p = 0.1-10$ Torr.

The following samples were used without further purification; Helium (Nippon Sanso, 99.9999%), Si_2H_6 (Toagosei Kagaku, >99.9%), Si_2H_6/He (Nippon Sanso, 1.03%), CCl_4 (Katayama Kagaku, 99%), O_2 (Nippon Sanso, 99.99%), H_2 (Nippon Sanso, 99.995%), and CH_3OH (Wako, 99.8%). Si_3H_8 was synthesized from SiH_4 using the electric discharge method.[10] The purity of Si_3H_8 synthesized was checked by a mass spectrometer.

3. Results

Mass Spectrometric Detection of Photoproducts. Si_2H_6/He was photolyzed by 193 nm laser light. The mass-selected ions at $m/z = 2$, 58, 60, and 92 were detected after 193 nm photolysis by electron impact ionization mass spectrometry combined with a near threshold ionization technique. The ionization potentials of observed molecules and the appearance potential of species produced from the ionization of Si_2H_6 are summarized in Table 2. Figure 1 shows the time profiles of ion signals. The rise time of the signals was faster than the time resolution of the detection systems, which is mainly controlled by the traveling time of molecules from the reaction zone in the photolysis cell to the ionization region.

TABLE 2: Ionization Potentials of Si Compounds and Appearance Potentials of Species Produced by Ionization of Si_2H_6[a]

molecule	ionization potential (eV)	appearance potential (eV)
SiH_3	8.14	11.0−11.9
$Si(H_2)Si$	8.2	11.4−11.8
$SiSiH_3$	<7.6	12.0−13.0
H_2SiSiH_2	8.1	10.0−10.9
H_3SiSiH	8.4	10.7−10.8
H_3SiSiH_2	7.6	11.2−11.6
Si_2H_6	9.7−10.2	
Si_3H_8	9.2	

[a] Ionization and appearance potentials are taken from ref 15b.

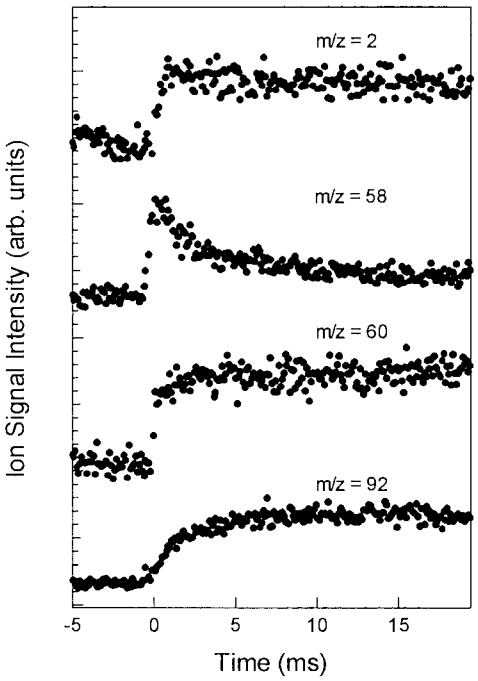

Figure 1. Time profiles of photoproducts after 193 nm photolysis of a Si_2H_6/He sample detected by using EI-MS: Si_2H_6 = 3 mTorr; p = 5 Torr. The ionization energies used are 15 (m/z = 2, H_2), 11 (m/z = 58, Si_2H_2), 10 (m/z = 60, Si_2H_4), and 16 eV (m/z = 92, Si_3H_8).

The ion signals at m/z = 2 and 92 could be regarded as stable products, since the time profiles did not show any decay. On the other hand, the time profile at m/z = 58 shows the fast decay, indicating that the species at m/z = 58 would be attributed to an unstable species. The peak height of the signal was found to be proportional to the Si_2H_6 concentration. It was also found that the decay profile could not be fitted to a single-exponential decay form. The decay curve consisted of a fast and a slow component, and the slow component depended on the total pressure. Further investigation will be required for elucidation of the decay processes.

The signal at m/z = 2 can be attributed to the H_2 molecule formed in the dissociation pathways summarized in Table 1. However, the quantitative measurements on H_2 detection could not be performed because of the low sensitivity of the H_2 signal and the large background signals at m/z = 2 caused by the high ionization energy (15 eV). The signal at m/z = 2 is possibly affected by the fragmentation of larger photolysis products.

It is known that disilene ($H_2Si{=}SiH_2$), which is a candidate for the signal at m/z = 60, has a high reactivity with polar molecules.[16] However, the time profile observed at m/z = 60 was not altered by the addition of H_2O, O_2, NO, and CH_3OH. These results suggested that disilene is not responsible for the signal at m/z = 60. Another possibility is silylsilylene (H_3SiHSi), an isomer of disilene. However, silylsilylene is known to be very reactive and its kinetic lifetime should be very short.[16] The ionization energy of 10 eV used in the detection of signal at m/z = 60 is higher than the ionization potential of Si_2H_6 (>9.7 eV) and Si_3H_8 (9.2 eV). In the ionization processes with higher ionization energy, the daughter ions may result from the fragmentation of higher mass molecules. To make sure the fragmentation occurred in the ionization processes, PI-MS was used to observe the mass-selected ions using lower ionization energies.

The ion signals at m/z = 31 (SiH_3^+), 58 ($Si_2H_2^+$), 59 ($Si_2H_3^+$), 60 ($Si_2H_4^+$), 61 ($Si_2H_5^+$), and 92 ($Si_3H_8^+$) were detected by using PI-MS at ionization energies of 8.9, 9.5, and 10.2 eV. Gas mixtures of Si_2H_6/He and CCl_4/ Si_2H_6/He were photolyzed by 193 nm light. The following sequential abstraction reactions were used as references in the identification of photoproducts:[15a]

$$CCl_4 + 193\ \text{nm} \rightarrow CCl_3 + Cl \quad (1)$$

$$Cl + Si_2H_6 \rightarrow Si_2H_5 + HCl, \quad Cl + Si_2H_5 \rightarrow Si_2H_4 + HCl, \quad \ldots (2)$$

Figure 2 shows the time profiles of the products after 193 nm photolysis of (a) Si_2H_6/He and (b) CCl_4/ Si_2H_6/He mixture gases.

The signals at m/z = 61 ($Si_2H_5^+$) were observed uniquely in the abstraction reactions as shown in Figure 2b, while no observation was confirmed in Si_2H_6 photolysis (Figure 2a).

The time profiles at m/z = 58 ($Si_2H_2^+$) were observed at the ionization energies of 8.9, 9.5, and 10.2 eV for both sample gases. Since it is expected that the fragmentation does not take place at the ionization energy of 8.9 eV, which is lower than the ionization potential of higher mass molecules such as Si_2H_6 and Si_3H_8, Si_2H_2 is assigned to a primary photoproduct. On the other hand, the signal at m/z = 60 ($Si_2H_4^+$) was only observed at the ionization energy of 10.2 eV, which is close to the appearance potential of Si_2H_4 produced from the ionization of Si_2H_6. From this fact, the signal at m/z = 60 is assigned to the products resulting from the fragmentation in the ionization processes of higher mass molecules. It is worth noting that although Si_2H_4 was postulated to be a key intermediate in low-temperature ArF LCVD of Si_2H_6,[7] present experimental results indicated that Si_2H_4 is not produced in 193 nm photolysis of Si_2H_6. The signal at m/z = 59 ($Si_2H_3^+$) was only detectable in the abstraction reactions, and Si_2H_3 formation in 193 nm photolysis would be ruled out.

The SiH_3^+ signal at m/z = 31 (IP = 8.14 eV) could not be observed for both gas samples except for the CCl_4/ Si_2H_6/He sample at the ionization energy of 10.2 eV. The detection limit of SiH_3 in our apparatus was evaluated from the reference reaction

$$Cl + SiH_4 \rightarrow HCl + SiH_3 \quad (3)$$

The yield for the production of SiH_3 radical for this reaction is known to be unity.[17] On the basis of the experimental conditions, the upper limit of SiH_3 formation in 193 nm photolysis of Si_2H_6 was estimated to be 0.03. Loh et al. reported the quantum yield for SiH_3 formation to be 0.05 ± 0.05.[17] Okada et al. reported that no signal due to SiH_3 radical has been detected using the REMPI method.[6] The results obtained in the present study are consistent with these reported results. The rate of wall loss of the SiH_3 radical in the reactor was measured to be 70−205 s^{-1},[11] which is much slower than the time resolution of the present

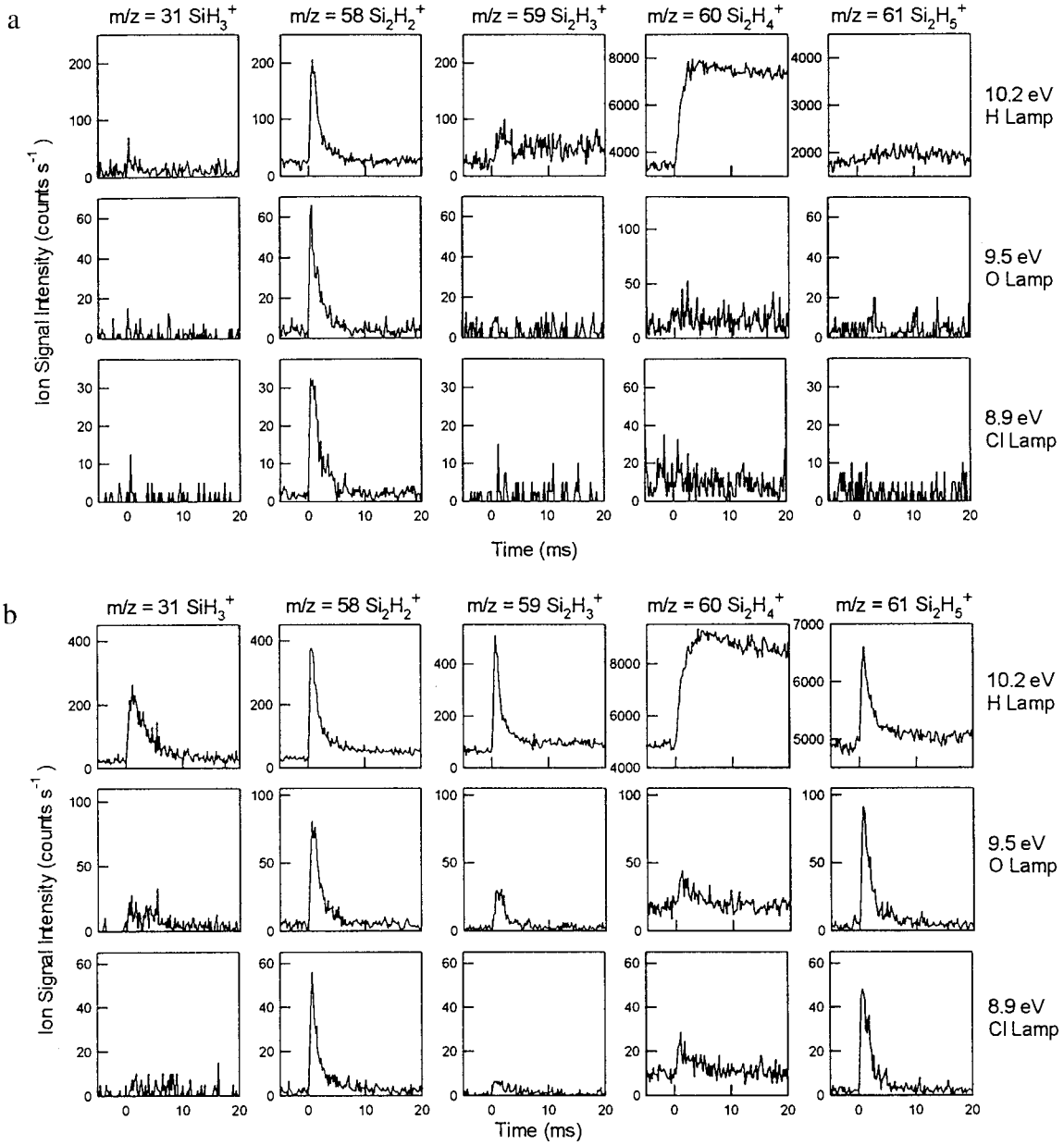

Figure 2. Time profiles of photoproducts after 193 nm photolysis of (a) Si_2H_6/He and (b) CCl_4/Si_2H_6/He samples detected by using PI-MS: CCl_4 = 10 mTorr; Si_2H_6 = 2.6 mTorr; p = 3.6 Torr.

apparatus. Therefore, the heterogeneous loss at the cell wall would not prevent the detection of SiH_3.

The signal at $m/z = 92$ assigned to Si_3H_8 (IP = 9.2 eV) was detected at the ionization energy of 10.2 eV both in the Si_2H_6/He and CCl_4/ Si_2H_6/He mixtures. However, $Si_3H_8^+$ was not detectable at the ionization energy of 9.5 eV due to the lower ionization efficiency.

Pathway of Si_3H_8 Formation. The ion signal at $m/z = 92$ was detected with EI-MS (Figure 1) and PI-MS (Figure 3). This signal can be assigned to Si_3H_8 formed by the following reaction:

$$SiH_2 + Si_2H_6\,(+\,M) \rightarrow Si_3H_8\,(+\,M) \qquad (4)$$

According to this mechanism, the formation of Si_3H_8 is inhibited if SiH_2 is trapped by a scavenger. To confirm this, H_2 was added to the constant partial pressure of Si_2H_6. The yield of Si_3H_8 was measured as a function of H_2 partial pressure.

$$SiH_2 + H_2\,(+\,M) \rightarrow SiH_4\,(+\,M) \qquad (5)$$

It is expected that the signal intensities of Si_3H_8 decrease with increasing H_2 concentration. With a steady-state assumption for SiH_2 for reactions 4 and 5, the following equations are obtained:

$$[Si_3H_8]_\infty = \frac{k_4[Si_2H_6]}{k_4[Si_2H_6] + k_5[H_2]}[SiH_2]_0 \qquad (6a)$$

$$\frac{1}{I} = \left\{1 + \frac{k_5}{k_4[Si_2H_6]}[H_2]\right\}\frac{C}{[SiH_2]_0} \qquad (6b)$$

where I is a signal intensity of Si_3H_8 at $t = \infty$ and k_4 and k_5 are the rates of reactions 4 and 5, respectively. C is the proportionality constant intrinsic to the detection system. The value of $C/[SiH_2]_0$ can be determined by the experiments with $[H_2] = 0$. The comparative experiments were performed by using EI-MS. The plots of $\xi = (1/I)\,([SiH_2]_0/C)$ vs $[H_2]$ are shown in Figure 4. The slope in eq 6 and in Figure 4 is the ratio of k_5 and k_4. The value of k_5/k_4 is estimated to be 8.53×10^{-4} at p = 5 Torr. The absolute rate constants of k_4 and k_5 were

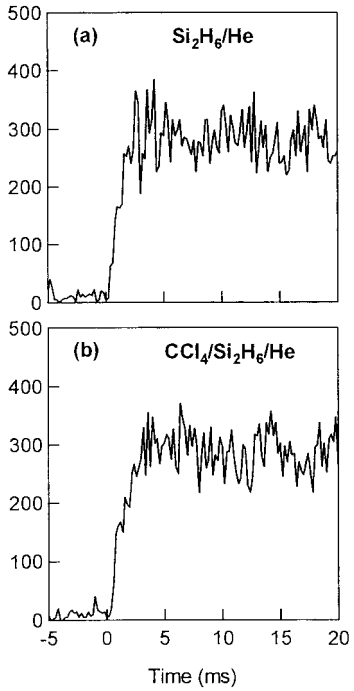

Figure 3. Time profiles of the ionization signal at $m/z = 92$ (Si_3H_8) after 193 nm photolysis of (a) Si_2H_6/He and (b) CCl_4/Si_2H_6/He samples detected by using PI-MS (the ionization energy used is 10.2 eV): CCl_4 = 10 mTorr; Si_2H_6 = 2.6 mTorr; p = 3.6 Torr.

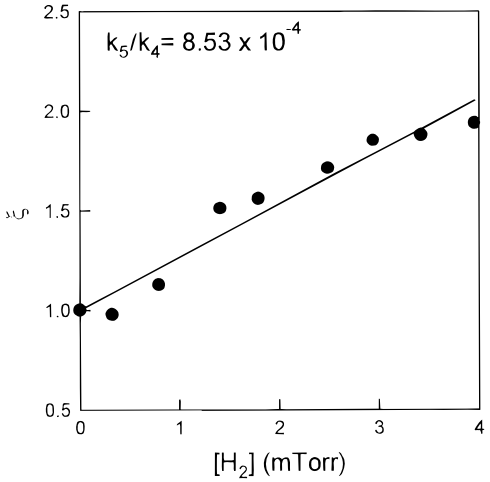

Figure 4. Plots of $\xi = (1/I)$ ($[SiH_2]_0/C$) as a function of H_2 concentrations. Circles are obtained with Si_2H_6 = 0.31 mTorr and p = 5 Torr. The line is a least-squares fit to the circles.

independently determined by Jasinski et al.,[9] from which the k_5/k_4 value is calculated to be 7.23×10^{-4}. This value is in reasonable agreement with our value obtained. Thus, this result strongly suggests that Si_3H_8 observed in the present study is exclusively generated from the reaction of SiH_2 with Si_2H_6 and SiH_2 is a primary photoproduct in 193 nm photolysis of Si_2H_6. Our determination of the quantum yield of SiH_2 is based on the quantitative measurements of the yield of Si_3H_8 ($m/z = 92$). However, there is some ambiguity on the rise rate of the signal at $m/z = 92$. As can be seen in Figure 1, the rise rate of the $m/z = 92$ ion signal is much slower than the production rate of Si_3H_8 predicted from the rate of the $SiH_2 + Si_2H_6$ reaction. Such slow rise rates of heavy molecules have also been observed in ArF laser photolysis of C_2Cl_4.[11] For example, the ion signal of C_2Cl_2 ($m/z = 94$) showed a rise time of about 3 ms, even though this radical was directly produced by the laser photolysis. This slow rise could be caused by the slow diffusion rate of the heavy

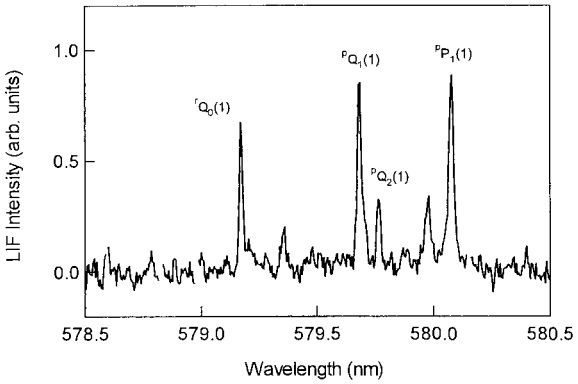

Figure 5. LIF excitation spectrum of SiH_2 produced in 193 nm photolysis, shown in the $\tilde{A}^1B_1(0,2,0) \leftarrow \tilde{X}^1A_1$ (0,0,0) band: Si_2H_6 = 17 mTorr. Line assignments are from refs 14 and 18.

molecule from the photolysis zone to the ionization chamber. In the present case, such slow diffusion processes can also be responsible for the slow rise rate of the ion signal at $m/z = 92$. On the other hand, the rise rate of the signal at $m/z = 60$ in Figure 1 seems to be much faster than the rate of diffusion, if we assume that the slow rise of the signal at $m/z = 92$ is cause by the diffusion. We can not resolve this discrepancy yet, but we also found that the rise rate of the mass signal varied with the laser alignment. If the diameter of the ArF laser beam is much smaller than the diameter of the reaction tube, the rise rate becomes slower, as expected, and if the laser beam is misaligned (e.g., laser beam hits the wall), the rise rate was found to be faster. In fact, the rise rates of the photoionization signal at $m/z = 60$ in Figure 2 observed with almost the same conditions show a slower rate than that in Figure 1, and it seems to be a "normal" rise rate. This difference could be caused by different laser alignment. These observations suggest that the origin of the slow rise of the mass signals at $m/z = 92$ (Figures 1 and 3) or $m/z = 60$ is not responsible for the chemical rate processes.

Because of this ambiguity on the rise rate of $m/z = 92$ (Si_3H_8), the assumption of the direct production of SiH_2 has to be confirmed by other evidence. Thus, the direct detection of SiH_2 was tried in 193 nm photolysis of Si_2H_6.

Figure 5 shows the LIF excitation spectrum of SiH_2 produced in 193 nm photolysis of 17 mTorr of Si_2H_6 without He buffer gas. The spectra are assigned to the transition in the $\tilde{A}^1B_1$ (0,2,0) $\leftarrow \tilde{X}^1A_1$ (0,0,0).[14,18] The time delay between the photolysis and probe laser pulses was set at 1.7 μs. The time profile monitored on the $^pP_1(1)$ line in the (0,3,0)−(0,0,0) band is shown in Figure 6. Absolute signal intensities rise within 500 ns. The decay rate could be controlled by the rate of reaction of SiH_2 with Si_2H_6.

Pseudo-first-order reaction rates have been obtained from single-exponential analysis of the decay of the time profile as a function of Si_2H_6 partial pressure. An example is shown in Figure 7 for the total pressure at 500 mTorr. The negligibly small intercept in the plots shown in Figure 7 is due to diffusion and experimental uncertainty. The absolute rate constants of SiH_2 with Si_2H_6 at 350 and 500 mTorr total pressure are $(1.3 \pm 0.3) \times 10^{-11}$ and $(3.3 \pm 1.7) \times 10^{-11}$ cm^3 molecule^{-1} s^{-1}, respectively. Jasinski et al.[9] reported the pressure dependence of the reaction rate constants of SiH_2 with Si_2H_6 in the range 1−10 Torr. Although the uncertainties of the present data are rather large, the pressure-dependent rate constants of the present results are consistent with the extrapolated values of Jasinski's data.

The evaluation of the quantum yield of Si_3H_8 formation was carried out by using EI-MS. The concentration of Si_3H_8

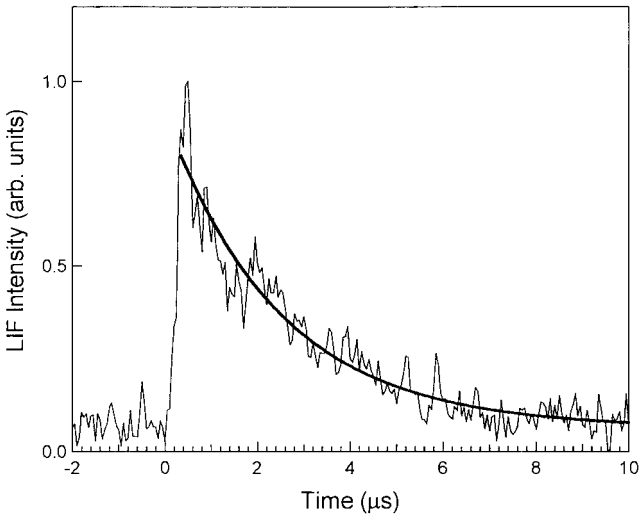

Figure 6. Time profile of the SiH_2 LIF signal $\tilde{A}^1B_1(0,3,0) \leftarrow \tilde{X}^1A_1(0,0,0)$: $Si_2H_6 = 100$ mTorr; $p = 500$ mTorr. The bold line is a single-exponential fit to the experimental data.

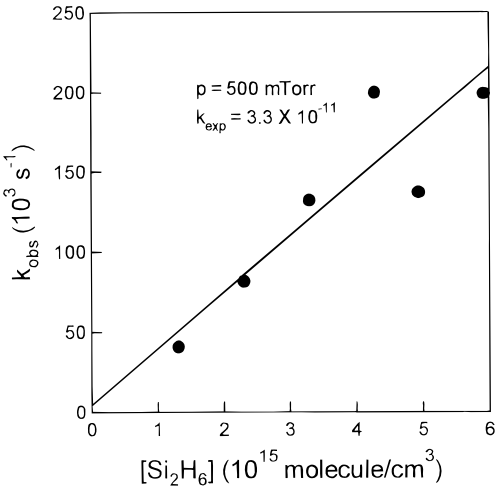

Figure 7. Pseudo-first-order decay rates of SiH_2 as a function of Si_2H_6 concentrations; Filled circles are obtained at $p = 500$ mTorr. The line is a least-squares fit to the circles.

produced in the reaction of $SiH_2 + Si_2H_6$ was estimated by comparing with a known amount of synthesized Si_3H_8 sample. We have confirmed that the laser power dependence of the ion signal at $m/z = 92$ on the photolysis laser is first order in the range 10−50 mJ/cm^2 per pulse. Figure 8 shows the results of the quantum yield measurements of Si_3H_8. No dependence on the Si_2H_6 precursor concentration was observed. The line shown in Figure 8 represents the average value of $\phi = 0.13 \pm 0.02$.

Measurement of Quantum Yield for H Atoms. H atoms produced from 193 nm photolysis of Si_2H_6 were observed by using the VUV-LIF method at 121.6 nm. The signal intensities were proportional to 193 nm laser intensities. The time profile of H atoms after 193 nm photolysis of Si_2H_6 did not show any decay ($t < 100$ μs). In the determination of the quantum yield of H atom formation, 193 nm photolysis of NH_3 was used as a reference.

$$NH_3 + 193\ \text{nm} \rightarrow H + NH_2 \qquad (7)$$

The quantum yield of H atom formation in this photodissociation is known to be 0.99.[19] Figure 9 shows the H atom concentration as a function of the Si_2H_6 concentration. The concentration of

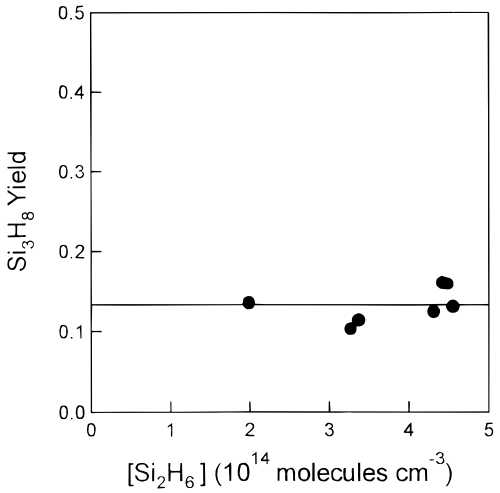

Figure 8. Quantum yield of Si_3H_8 produced by the $SiH_2 + Si_2H_6$ reaction: $p = 5$ Torr. The line represents an average value of the quantum yield per quantum absorbed; $\phi = 0.13 \pm 0.02$.

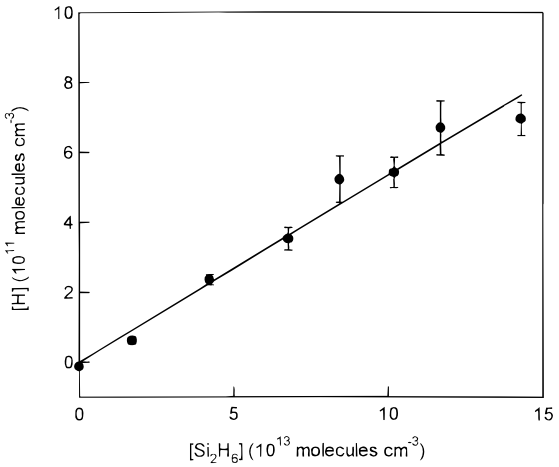

Figure 9. Plots H atom concentration as a function of Si_2H_6 concentration. Filled circles represent experimental results. The line represents the quantum yield of H per quantum absorbed; $\phi = 0.09 \pm 0.01$.

H atom was proportional to that of Si_2H_6. From this figure, the quantum yield of H atom formation in 193 nm photolysis of Si_2H_6 was estimated to be 0.09 ± 0.01.

4. Discussion

Primary Processes. *Formation of Si_2H_2.* There are two low-lying isomers of Si_2H_2. The nonplanar double-bridged $Si(H_2)Si$ structure is the most stable in Si_2H_2 conformations, and silasilene ($H_2Si{=}Si$:) is found to be 14.9 kcal/mol less stable than the double-bridged structure.[20] As seen in Figures 1 and 2a, Si_2H_2 is identified as a primary photoproduct, and the following reactions are possible according to Table 1:

$$Si_2H_6 + 193\ \text{nm} \rightarrow Si(H_2)Si + 2H_2 \qquad (r4)$$

$$\rightarrow H_2Si{=}Si: + 2H_2 \qquad (r6)$$

These reactions effectively produce H_2 molecules.

Formation Channels of H and SiH_4. The following six H atom formation channels need to be considered.

$$Si_2H_6 + 193\ nm \rightarrow H_3SiSiH_2 + H \quad (r7)$$

$$\rightarrow SiH_3 + SiH_2 + H \quad (r10)$$

$$\rightarrow SiH_4 + SiH + H \quad (r12)$$

$$\rightarrow H_2SiSiH + H_2 + H \quad (r13)$$

$$\rightarrow H_2SiSiH_2 + 2H \quad (r14)$$

$$\rightarrow Si(H)Si + 2H_2 + H \quad (r15)$$

It should be noted that the pair-products of H atom are ground-state products. Since neither Si_2H_3 nor Si_2H_4 were observed in 193 nm photolysis, reactions r13 and r14 are ruled out for H atom formation. Reaction r7 will be unlikely since a $Si_2H_5^+$ signal was not detectable by the mass spectrometric techniques. Since the heat of reaction of the Si(H)Si production channel (r15) is slightly higher than the photon energy at 193 nm (148 kcal/mol) and a Si_2H^+ signal could not be observed by the mass spectrometric techniques, this channel can also be ruled out. We next consider a contribution of reaction r10 to H atom formation. In the present photolysis experiment, no SiH_3 radical has been detected ($\phi < 0.03$). On the basis of on this fact, it is seen that reaction r12 is the major channel in H atom formation and the contribution of reaction r10 to H atom formation is negligibly small.

The quantum yield of SiH_4 formation has been estimated to be 0.1 by Chu et al.[1] There are three SiH_4 formation channels in the ground-state products as follows:

$$Si_2H_6 + 193\ nm \rightarrow SiH_4 + SiH_2 \quad (r2)$$

$$\rightarrow SiH_4 + Si + H_2 \quad (r8)$$

$$\rightarrow SiH_4 + SiH + H \quad (r12)$$

Okada et al.[6] reported a quantum yield of ground-state Si(^{3}P) atom formation of 0.01, from which the quantum yield of the $SiH_4 + Si + H_2$ channel is expected to be less than 0.01. Since the branching of reaction r12 is roughly expected to be 0.09 on the basis of the H atom yield, the sum of branching of reactions r8 and r12 is approximately equal to 0.1. According to this branching fraction, reaction r2 is eliminated in 193 nm photolysis. Begemann et al. observed a SiH LIF signal and suggested that no excess SiH ground state is produced in 193 nm photodissociation of Si_2H_6.[21] The quantum yield of SiH (0.09) is consistent with the results of Chu et al. in that they propose that production of SiH and SiH_2 is less than 20%.[1] Although there exist four SiH_4 formation channels coupled with the excited-state products (Table 1), the contribution of the excited-state channels to the SiH_4 formation may be unimportant according to the branching fractions discussed above.

Formation of SiH_2. The rise time of SiH_2 formation, approximately 500 ns, has also been observed in collision-free conditions (Figure 6). The slow formation of photoproducts has been observed in 157 nm photolysis of SiH_4 and GeH_4[22] and in 193 nm photolysis of aromatic molecules.[23] Analogous to these cases, the slow formation might be assigned to an electronic relaxation from the photoprepared excited state to the ground state followed by dissociation of the ground state.

$$Si_2H_6 + 193\ nm \rightarrow Si_2H_6^* \rightarrow Si_2H_6^{\ddagger} \rightarrow SiH_2 + \text{other products}$$

where * and ‡ indicate electronically excited and hot molecular states, respectively. It is considered that the rise time reflects probably a long unimolecular dissociation lifetime of $Si_2H_6^{\ddagger}$.

The following three ground-state channels are opened for SiH_2 formation:

$$Si_2H_6 + 193\ nm \rightarrow SiH_4 + SiH_2 \quad (r2)$$

$$\rightarrow 2SiH_2 + H_2 \quad (r9)$$

$$\rightarrow SiH_3 + SiH_2 + H \quad (r10)$$

Since reactions r2 and r10 are eliminated as discussed above, reaction r9 is a plausible mechanism for SiH_2 formation. The quantum yield of SiH_2 formation can be assumed to be equal to that of Si_3H_8 (0.13 ± 0.02), since SiH_2 reacts with Si_2H_6 to form Si_3H_8 without the side reactions (Figure 7).

For the formation of excited SiH_2, the following three reactions need to be considered:

$$Si_2H_6 + 193\ nm \rightarrow SiH_4 + SiH_2\ (\tilde{a}^3B_1) \quad (r17)$$

$$\rightarrow SiH_4 + SiH_2\ (\tilde{A}^1B_1) \quad (r18)$$

$$\rightarrow SiH_2\ (\tilde{a}^3B_1) + SiH_2 + H_2 \quad (r20)$$

Eres et al.[2] proposed reaction r18 based on the observation of fluorescence assigned to SiH_2 ($\tilde{A}^1B_1 - \tilde{X}^1A_1$). According to our interpretation of SiH_4 formation, reactions r17 and r18 should be minor. If Si_2H_6 molecules are exited to the triplet state at 193 nm,[24] reaction r20 is allowed based on the spin selection rule. Although both reactions r9 and r20 can be responsible for SiH_2 production, we prefer reaction r9 since the absorption cross section of Si_2H_6 at 193 nm seems to be too large for the singlet to triplet transition.

TABLE 3: Summary of Proposed Dissociation Pathways and its Branching Fractions in 193 nm Photolysis of Si_2H_6

dissociation pathway	Φ	ref
$Si_2H_6 + 193\ nm \rightarrow$ products	0.7[a]	1
$\rightarrow SiH_4 + Si + H_2$	$\sim$0.01[b]	6
$\rightarrow SiH_4 + SiH + H$	0.09[b]	this work
$\rightarrow 2SiH_2 + H_2$, $SiH_2(\tilde{a}^3B_1) + SiH_2 + H_2$	0.13	this work
$\rightarrow 2SiH_3$, $SiH_3 + SiH_2 + H$	$<$0.03[c]	this work
$\rightarrow Si(H_2)Si + 2H_2$	++[d]	this work
$\rightarrow H_2SiSi + 2H_2$	++[d]	this work

[a] Dissociation quantum yield. [b] Quantum yield of SiH_4 formation was estimated to be 0.1 in ref 1. [c] Values represent the upper limit of formation. [d] Expected to be main channel. See text in detail.

Dissociation Pathways. The product branching fractions proposed in the present study are summarized in Table 3. Perkins et al.[10] reported that 147 nm photolysis of Si_2H_6 resulted in the formation of H_2, SiH_4, Si_3H_8, Si_4H_{10}, Si_5H_{12}, and a solid hydridic silicon film. These products were explained by assuming the following primary processes:

$$Si_2H_6 + 147\ nm \rightarrow SiH_2 + SiH_3 + H$$

$$\rightarrow SiH_3SiH + 2H$$

$$\rightarrow Si_2H_5 + H$$

It is noted that H atoms are produced in three reaction channels. On the other hand, in 193 nm photolysis, the quantum yield of H atom formation is only 0.09.

The electronic spectral properties of Si_2H_6 have been studied by synchrotron radiation,[25] ab initio calculations,[26] and electron energy loss spectroscopy (EELS).[23] The synchrotron radiation study concluded that the first band of the vacuum UV electronic

spectrum is a A_{1g} (4s) ← A_{1g} Rydberg transition, which is symmetry forbidden, and the second peak at 147 nm is assigned to a A_{2u} (4p) ← A_{1g} Rydberg transition. On the other hand, a theoretical study allowed the unambiguous assignment of the first band to an allowed A_{2u} (4p) Rydberg excitation. In the EELS study, the lowest transition (~6.3 eV) has been identified as the A_{1g} (4s) ← A_{1g} triplet transition. Although the nature of optical transition is still uncertain, it seems that the differences between 147 and 193 nm photochemistry reflect the photoexcited-state characters. The higher Rydberg and dissociative valence states will be prepared by 147 nm photoexcitation.

Five H_2 elimination channels are concluded to be important in 193 nm photolysis, as seen in Table 3. It is well-known that the primary processes in 147 nm photolysis of C_2H_6 are H_2 elimination channels.[27] The optical transition of C_2H_6 at 147 nm has been assigned to the transition to 3s and/or 3p Rydberg states, which can be the same transition as Si_2H_6 at 193 nm.

$$C_2H_6 + 147\ \text{nm} \rightarrow C_2H_6^* \rightarrow C_2H_4‡ + H_2 \rightarrow C_2H_2 + 2H_2$$

Analogous to the case of C_2H_6, the H_2 elimination is expected to be dominant in 193 nm photolysis of Si_2H_6. The sum of branching fractions of SiH_2 and SiH_4 is evaluated to be <0.3; therefore, Si_2H_2, which is the pair product of the H_2 molecule, seems likely to be a main photoprocuct in the silicon-containing molecules. Jasinski observed transient absorption in the wavelength range 333.6−363.8 nm following 193 nm photolysis of Si_2H_6.[5] They concluded that at least two transient species, each of which contains two silicon atoms, are responsible for the absorption. One of the transient species is assigned as H_2SiSiH_2. The assignment of the second species is to a silylene or silylidyne isomer from the set of molecules SiH_x for $x = 2-4$. A part of the assignments, Si_2H_2, is in reasonable agreement with the transient species at $m/z = 58$ observed in the present study. On the other hand, the results of PI-MS experiments indicate that H_2SiSiH_2 may be not produced in the photolysis. Clearly, further work is needed to clarify the origin of the absorption observed by Jasinski. The measurement of the absorption spectra around 330−360 nm is highly desirable. The quantitative measurements for H_2 and Si_2H_2 are necessary for further discussion of the dissociation mechanism.

5. Conclusion

We have performed the detection of photoproducts by time-resolved mass spectrometry and laser-induced fluorescence techniques in order to deduce the primary photodissociation mechanism of Si_2H_6 at 193 nm. Si_2H_2, SiH_2, and H could be detected as primary photoproducts in 193 nm photolysis and the quantum yields of SiH_2 and H were estimated. Detection of SiH_3, Si_2H_4, and Si_2H_5 produced in 193 nm photolysis was also attempted, but no signal has been detected. By combining with the existing data, it was suggested that H_2 elimination processes are important in 193 nm photolysis of Si_2H_6.

References and Notes

(1) Chu, J. O.; Begemann, M. H.; McKillop, J. S.; Jasinski, J. M. *Chem. Phys. Lett*. **1989**, *155*, 576.
(2) Eres, D.; Geohegan, D. B.; Lowndes, D. H.; Mashburn, D. N. *Appl. Surf. Sci.* **1989**, *36*, 70.
(3) Muranaka, Y.; Motooka, T.; Lubben, D.; Green, J. E. *J. Appl. Phys.* **1989**, *66*, 910.
(4) Boch, E.; Fuchs, C.; Fogarassy, E.; Siffert, P. *Appl. Surf. Sci.* **1989**, *43*, 17.
(5) Jasinski, J. M. *Chem. Phys. Lett.* **1991**, *183*, 558.
(6) Okada, T.; Nishimi, A.; Shibamaru, N.; Maeda, M. *Jpn. J. Appl. Phys.* **1992**, *31*, 3707.
(7) Flwler, B.; Lian, S.; Krishnan, S.; Jung, L.; Li, C.; Samara, D.; Manna, I.; Banerjee, S. *J. Appl. Phys.* **1992**, *72*, 1137.
(8) Stafast, H. *Appl. Phys. A* **1988**, *45*, 93.
(9) Jasinski, J. M.; Chu, J. O. *J. Chem. Phys.* **1988**, *88*, 1678.
(10) Perkins, G. G. A.; Lampe, F. W. *J. Am. Chem. Soc.* **1979**, *101*, 1109.
(11) Matsumoto, K.; Koshi, M.; Okawa, K.; Matsui, H. *J. Phys. Chem.* **1996**, *100*, 8796.
(12) Miyoshi, A.; Yamauchi, N.; Matsui, H. *J. Phys. Chem.* **1996**, *100*, 4893.
(13) Murakami, Y.; Koshi, M.; Matsui, H.; Kamiya, K.; Umeyama, H. *J. Phys. Chem.* **1996**, *100*, 17501.
(14) (a) Dubois, I. *Can. J. Phys.* **1968**, *46*, 2485. (b) Inoue, G.; Suzuki, M. *Chem. Phys. Lett.* **1985**, *122*, 361. (c) Fukushima, M.; Mayama, S.; Obi, K. *J. Chem. Phys.* **1992**, *96*, 44.
(15) (a) Ruscic, R.; Berkowitz, J. *J. Chem. Phys.* **1991**, *95*, 2407. (b) Ruscic, R.; Berkowitz, J. *J. Chem. Phys.* **1991**, *95*, 2416. (c) Curtiss, L. A.; Raghavachari, K.; Deutsch, P. W.; Pople, J. A. *J. Chem. Phys.* **1991**, *95*, 2433.
(16) Jasinski, J. M.; Becerra, R.; Walsh, R. *Chem. Rev.* **1995**, *95*, 1203. Becerra, R.; Walsh, R. *Research in Chemical Kinetics III*; Compton, G., Walsh, R., Eds.; Elsevier: Amsterdam, 1996; p 263.
(17) Loh, S. K.; Jasinski, J. M. *J. Chem. Phys.* **1991**, *95*, 4914.
(18) Inoue, G.; Suzuki, M. *Chem. Phys. Lett.* **1985**, *122*, 361.
(19) Kenner, R. D.; Rohrer, F.; Stuhl, F. *J. Chem. Phys.* **1987**, *86*, 2036.
(20) Ho, P.; Coltrin, M. E.; Binkley, J. S.; Melius, C. F. *J. Phys. Chem.* **1986**, *90*, 3399.
(21) Begemann, M. H.; Dreyfus, R. W.; Jasinski, J. M. *Chem. Phys. Lett.* **1989**, *155*, 351.
(22) Tonokura, K.; Mo, Y.; Matsumi, Y.; Kawasaki, M. *J. Phys. Chem.* **1992**, *96*, 6688.
(23) Tsukiyama, K.; Bersohn, R. *J. Chem. Phys.* **1987**, *86*, 747. Yi, W.; Chattopadhyay, A.; Bersohn, R. *J. Chem. Phys.* **1991**, *94*, 5994.
(24) Dillon, M. A.; Spence, D.; Boesten, L.; Tanaka, H. *J. Chem. Phys.* **1988**, *88*, 4320.
(25) Itoh, U.; Toyoshima, Y.; Onuki, H.; Washida, N.; Ibuki, T. *J. Chem. Phys.* **1986**, *85*, 4867.
(26) Gelizé, M.; Dargelos, A.; Márquez, A.; Sanz, J. F. *Chem. Phys.* **1991**, *149*, 319.
(27) McNesby, J. R.; Okabe, H. *Adv. Photochem.* **1964**, *3*, 157. Hampson, R. F., Jr.; McNesby, J. R. *J. Chem. Phys.* **1965**, *42*, 2200.